J Solid State Electrochem (2012) 16:2267–2273
DOI 10.1007/s10008-012-1665-z

ORIGINAL PAPER

Modified electrodes with Keggin-type silicotungstates and poly(brilliant cresyl blue)

**Diana M. Fernandes · Christopher M. A. Brett ·
Ana M. V. Cavaleiro**

Received: 21 November 2011 / Revised: 15 January 2012 / Accepted: 21 January 2012 / Published online: 8 February 2012

Abstract Electrosynthesis of poly(brilliant cresyl blue) in aqueous solution in the presence of Keggin-type polyoxotungstates, $[SiW_{11}Fe(H_2O)O_{39}]^{5-}$ or $[SiW_{11}Co(H_2O)O_{39}]^{6-}$, was used to prepare modified glassy carbon electrodes. The deposited hybrid organic/inorganic films were studied and characterised by cyclic voltammetry and electrochemical impedance spectroscopy. Cyclic voltammetry showed that the electrochemical features of the polyoxoanions were maintained after immobilisation, with the first tungsten reduction peak involving the uptake of protons from the solution. The chemically modified electrodes were stable, and their preparation was easy to perform. The results provide valuable information for exploring future applications of these films in electrochemical sensors or electrocatalysis.

Keywords Keggin-type polyoxotungstates · Glassy carbon · Brilliant cresyl blue · Electropolymerisation · Polyoxometalates

---

D. M. Fernandes · A. M. V. Cavaleiro (✉)
Department of Chemistry/CICECO, University of Aveiro,
3810-193 Aveiro, Portugal
e-mail: anacavaleiro@ua.pt

C. M. A. Brett
Department of Chemistry, Faculty of Science and Technology,
University of Coimbra,
3004-535 Coimbra, Portugal

D. M. Fernandes
REQUIMTE/Department of Chemistry and Biochemistry,
Faculty of Science, University of Porto,
4169-007 Porto, Portugal

Introduction

Polyoxometalates (POMs) represent a unique class of inorganic compounds with applications in catalysis, medicine, electrochemistry, analytical chemistry, materials science, energy storage and optics [1–20]. Keggin-type POM anions are known for their ability to accept a large number of electrons, giving rise to mixed-valence species, which makes them very attractive for chemically modified electrodes and electrocatalysis [1, 11].

Immobilising redox-active POMs onto electrodes simplifies the study of their electrochemistry and facilitates their application. Several strategies have been developed to prepare chemically modified electrodes with a variety of POMs [1, 21–26]. The layer-by-layer (LbL) method is one of the most common, and many examples of its application in the preparation of POM materials have been reported [1, 21, 25–32]. Another strategy is based on POM entrapment into polymer matrices prepared by the electrochemical polymerisation (in the presence of the POM) of the corresponding monomer on the electrode surface, for example, by cyclic voltammetry. This leads to the formation of modified electrodes containing a hybrid organic–inorganic film in which the POM and the polymer may interact electrostatically. Most reported studies use Keggin-type polyoxometalates, $[XM_{12}O_{40}]^{n-}$ anions (X = P, Si; M = Mo, W) with conducting polymers, such as polypyrrole [33, 34], polyaniline [35, 36] or polythiophene and their derivatives [8, 22, 37–39].

Azine dyes can also be used to prepare modified electrodes by electrochemical polymerisation: polyphenazine and polyphenoxazine redox polymers can be conducting polymers as well as redox mediators [40, 41]. Brilliant cresyl blue (BCB) is a cationic quinone–imine dye with a planar and rigid structure, and poly(brilliant cresyl blue) (PBCB) has been used in the production of electrochemical biosensors [41, 42]. The insertion of POMs in this type of cationic polymer can lead to hybrids whose properties may be explored in modified electrodes. BCB–polyoxometalate films have been prepared by the LbL method and their thermal and photochemical properties have been studied [43]. To our knowledge, films of PBCB and polyoxometalates have not been previously described.

The present work concerns the preparation and electrochemical characterisation of PBCB-modified electrodes doped with $[SiW_{11}Fe^{III}(H_2O)O_{39}]^{5-}$ ($SiW_{11}Fe$) and $[SiW_{11}Co^{II}(H_2O)O_{39}]^{6-}$ ($SiW_{11}Co$). The two polyoxotungstates differ in that they contain substituting metals with different redox activities. The electrochemical behaviour of the immobilised POMs was examined by cyclic voltammetry. The modified electrodes were also characterised by electrochemical impedance spectroscopy. This work follows our interest in electrode modification with first-row transition metal-substituted Keggin-type phosphotungstates and silicotungstates [23–26, 44, 45], probing possible electrocatalytic effects, and in the preparation of sensors with PBCB [42].

Experimental section

Reagents and solutions

Acetic acid (Pronalab), sodium acetate (Carlo Erba) and brilliant cresyl blue (Fluka) were used as received. The potassium salts of the α-Keggin silicotungstates $K_5[SiW_{11}Fe^{III}(H_2O)O_{39}]\cdot 13H_2O$ and $K_6[SiW_{11}Co^{II}(H_2O)O_{39}]\cdot 12H_2O$ were prepared by previously published procedures [46, 47] and characterised by thermal and elemental analysis, as well as by infrared spectroscopy. The results were in agreement with previously published values [47].

Electrolyte solutions for voltammetry were prepared using ultrapure water (resistivity, 18.2 MΩ cm at 25 °C; Direct-Q 3 UV system, Millipore). Buffer solutions in the pH range of 3.0–4.5 were prepared by mixing appropriate amounts of CH_3COOH (0.1 M) and $NaCH_3COO$ (0.1 M) solutions; buffer solution H_2SO_4/Na_2SO_4 pH 3.0 was prepared by mixing H_2SO_4 (0.1 M) and Na_2SO_4 (0.1 M).

Freshly prepared solutions, deoxygenated with pure nitrogen for at least 10 min, were used for film preparation. Solutions used for electrochemical characterisation were also deoxygenated with nitrogen for 10 min.

Instrumentation and methods

Cyclic voltammetry experiments were carried out using a computer-controlled potentiostat (PGSTAT-12/GPES software from Autolab/Ecochemie, Netherlands). A conventional three-electrode compartment cell was used. The auxiliary and reference electrodes were platinum wire (7.5 cm; BAS, MW-1032) and Ag/AgCl (sat. KCl) (BAS, MF-2052), respectively. The working electrode was a glassy carbon electrode (GCE) (3-mm diameter; BAS, MF-2012).

Electrochemical impedance measurements were carried out using a Solartron 1250 frequency response analyser, coupled to a Solartron 1286 electrochemical interface (UK) controlled by ZPlot 2.4 software. The voltage perturbation was 10 mV rms over a frequency range from 65 kHz to 0.1 Hz with 10 frequencies per decade and 60 s integration time. Impedance spectra were analysed by fitting equivalent electrical circuits using ZView 3.2 software (Scribner Associates, NC, USA). A combined glass electrode (Hanna Instruments HI 1230) connected to an Inolab pH level 1 pH meter was used for the pH measurements.

Preparation of POM-doped PBCB films

Prior to coating, the GCE was conditioned by a polishing/cleaning procedure. The GCE was successively polished with 1.0 μm diamond polishing compound (Metadi II, Buehler) and aluminium oxide of particle size 0.3 μm (Buehler-Masterprep) on a microcloth polishing pad (BAS Bioanalytical Systems Inc.), then the electrode was rinsed with ultrapure water and finally sonicated for 5 min in an ultrasonic bath (Branson 2510). Electrochemical pretreatment of the electrode was performed by performing 20 consecutive potential scans, between −0.8 and 0.8 V, at a scan rate of 100 mV s^{-1} in NH_4Ac/HCl (pH 3.4; 1.0 M NH_4Ac/0.5 M HCl) buffer solution.

Unless otherwise stated, POM-doped PBCB films were prepared by potential cycling (5 cycles) at 50 mV s^{-1} between −0.98 and +1.00 V vs Ag/AgCl in 0.25 mM $SiW_{11}Fe$ or $SiW_{11}Co$/0.1 mM BCB/pH=4.0 acetate buffer solutions containing 0.1 M KNO_3. Before each use, the electrode was rinsed with ultrapure water. All measurements were made at room temperature (~25 °C).

Results and discussion

Film formation and stability

The electrodeposition of PBCB films doped with Keggin-type polyoxotungstates on glassy carbon electrodes was carried out by potential cycling in aqueous solutions containing the chosen POM ($SiW_{11}Fe$ or $SiW_{11}Co$) and BCB. All film formation experiments were done in acidic aqueous solutions since the silicotungstates used in this work are unstable in neutral and basic aqueous solution. The potential cycling electropolymerisation leads to polyphenazine film thicknesses of the order of 1 μm depending on the polymer film structure and morphology and on the counterion identity [48]. According to previously published studies [40–42], polymerisation begins by the irreversible oxidation of the monomer and the formation of radical cations. Binding may occur through the amino group or by ring-to-ring coupling [40–42].

In order to optimise the electropolymerisation conditions, the influence of various parameters was studied: monomer and polyoxometalate concentration, pH and supporting electrolyte and possible catalysis from nitrate ions in the supporting electrolyte. Solution compositions used for film preparation are summarised in Table 1.

It has been demonstrated that the buffer solution pH has a significant influence on polymer film formation and that nitrate ions in the supporting electrolyte accelerate the polymer growth rate [42]. To evaluate the influence of pH, the formation of $SiW_{11}Fe$ POM-doped PBCB films was carried out in 0.1 M acetate buffer solutions at pH 3.0 and 4.0 (Table 1). Increasing the pH by 1 unit led to an increase of 25% in the height of the tungsten reduction peaks in the absence of nitrate (solution compositions 1 and 4, Table 1) and of 72% when nitrate (0.1 M) is present (2 and 6, Table 1). At pH 3.0, no significant difference resulted from using H_2SO_4/Na_2SO_4 or acetate buffer solutions (1 and 3, Table 1). Addition of KNO_3 to pH 4.0 acetate buffer (4 and 6, Table 1) led to a 43% increase in the height of the tungsten reduction peaks, while in similar experiments at pH 3.0 (1 and 2, Table 1), this change was only 4.2%.

Increasing the BCB monomer concentration in pH 4 buffer solution from 0.10 to 0.25 mM, for each of the three $SiW_{11}Fe$ POM concentrations used (6 and 9, 7 and 10 and 8 and 11, Table 1), led to an increase in the I_{pc} values for the first tungsten reduction peak of 14%, 43% and 24%, respectively. This can be explained by the fact that the rate of polymerisation initiation is faster at higher concentrations of monomer which leads to thicker and more porous polymer films that incorporate a larger quantity of POM. However, these films were not very stable, and on the day after film preparation, the I_{pc} values were 21–28% lower. For the same concentration of BCB and different POM concentrations (9, 10 and 11, Table 1), the highest peak currents were found for 0.25 mM. This implies that a high concentration of POM does not facilitate its incorporation into the polymer film.

A similar study performed with the $SiW_{11}Co$ anion showed no significant differences compared with that of the $SiW_{11}Fe$. Consequently, the conditions chosen for the preparation of POM-doped PBCB films were 0.10 mM BCB, 0.25 mM POM, pH 4.0 0.1 M acetate buffer and 0.1 M KNO_3.

Cyclic voltammetry characterisation of the POM-doped PBCB films

Previous voltammetric studies of $SiW_{11}Fe$ and $SiW_{11}Co$ in aqueous solution (pH range, 2.0–4.5) indicated that both compounds originate two reversible or quasi-reversible two-electron consecutive waves at negative potentials, corresponding to the reduction of W^{VI}. Another wave at a less negative potential, for $SiW_{11}Fe$, is due to the redox process of $Fe^{III/II}$ [23]. Both give E_{pa} and E_{pc} values independent of scan rate, thus showing reversible electrode reactions; peak currents are proportional to the square root of scan rate (linear plots with $0.999 \geq r \geq 0.992$), corresponding to diffusion-controlled redox processes [23, 49].

The cyclic voltammograms shown in Figs. 1 and 2 were obtained for GCEs modified with PBCB films doped with $SiW_{11}Fe$ and $SiW_{11}Co$ at different scan rates and at pH 3.5 and 4.0, respectively. Two close-to-reversible waves are observed at potentials more negative than −0.5 V, due to the reduction of W^{VI}, and the values of $E_p - E_{p/2}$ between 27 and 36 mV for the two W waves each correspond to two-electron processes. Thus, the electrochemical properties of the two POMs studied are maintained in the films. The pair

Table 1 Composition of the solutions used for the preparation of the iron silicotungstate-doped PBCB-modified electrodes, and values of j_{pc} for the first tungsten reduction peak measured from the cyclic voltammogram of $SiW_{11}Fe$ at 100 mV s^{-1} in pH 4.0, 0.1 M acetate buffer

Solution composition	BCB (mM)	POM (mM)	Buffer electrolyte	KNO_3 (M)	j_{pc} (μA cm^{-2})
1	0.10	0.10	Acetic acid/acetate, pH 3.0	0	−3.3
2	0.10	0.10	Acetic acid/acetate, pH 3.0	0.10	−3.4
3	0.10	0.10	H_2SO_4/Na_2SO_4, pH 3.0	0	−3.3
4	0.10	0.10	Acetic acid/acetate, pH 4.0	0	−4.1
5	0.10	0.25	Acetic acid/acetate, pH 4.0	0	−4.7
6	0.10	0.10	Acetic acid/acetate, pH 4.0	0.10	−5.9
7	0.10	0.25	Acetic acid/acetate, pH 4.0	0.10	−6.8
8	0.10	0.50	Acetic acid/acetate, pH 4.0	0.10	−6.2
9	0.25	0.10	Acetic acid/acetate, pH 4.0	0.10	−6.8
10	0.25	0.25	Acetic acid/acetate, pH 4.0	0.10	−9.7
11	0.25	0.50	Acetic acid/acetate, pH 4.0	0.10	−7.9

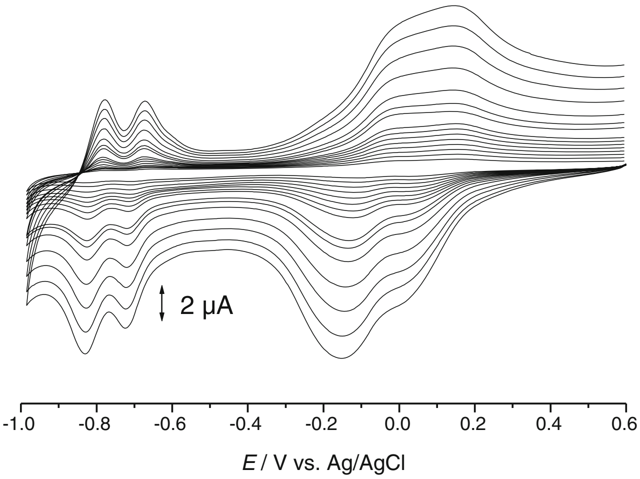

Fig. 1 Cyclic voltammograms of $SiW_{11}Fe$-doped PBCB-modified electrodes in pH 3.5 acetate buffer solution at scan rates of 20, 30, 40, 50, 60, 70, 80, 90, 100, 120, 150, 200, 250, 300 and 350 mV s^{-1}

of peaks for the one-electron reduction/oxidation of $Fe^{III/II}$ was not visible because PBCB exhibits oxidation/reduction peaks at almost the same potential [42].

In the experimental timescale employed (scan rates in the range of 20–350 mV s^{-1}), the values of peak potential changed only slightly with scan rate, and the ratio of the magnitude of oxidation to reduction peak currents is in the range of 0.97–1.00. The cathodic and anodic peak currents are directly proportional to scan rate (linear plots with $0.997 \geq r \geq 0.994$), which indicate surface-confined processes. Similar behaviour was observed for these metal-substituted POMs immobilised by electropolymerisation with poly(3,4-ethylenedioxythiophene) (PEDOT) and by the layer-by-layer methodology using poly(ethylenimine) [25, 26, 44].

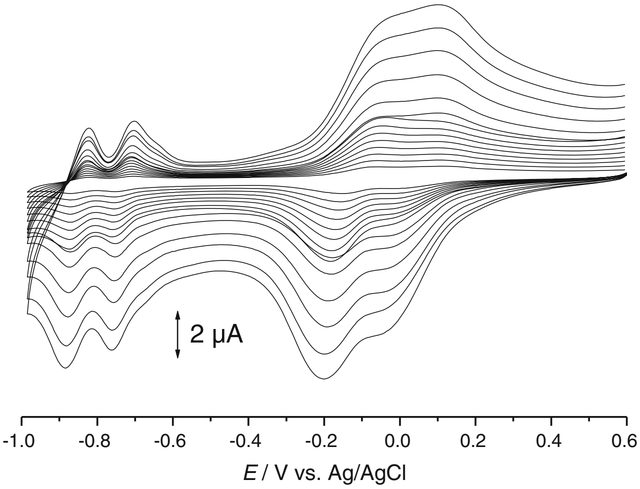

Fig. 2 Cyclic voltammograms of $SiW_{11}Co$-doped PBCB-modified electrodes in pH 4.0 acetate buffer solution at scan rates of 20, 30, 40, 50, 60, 70, 80, 90, 100, 150, 180, 200, 250, 300 and 350 mV s^{-1}

Surface coverage (Γ) can be estimated approximately from cyclic voltammetry according to the equation for reversible surface-confined species $\Gamma = (4I_{pa}RT) / (n^2F^2\nu A)$ where I_{pa} is the anodic peak current (amperes), n is the number of electrons transferred (two in this case), ν is the scan rate (V s^{-1}), A is the geometric area of the electrode (0.0725 cm^2), R is the gas constant, T is the temperature (298 K) and F is the Faraday constant [25, 26]. Peak currents for the first tungsten reduction were plotted against scan rate (20–350 mV s^{-1}), and the value of I_{pa}/ν obtained was used to calculate the surface coverage. This led to a surface coverage of $2.9 \pm 0.4 \times 10^{-11}$ mol cm^{-2} for $SiW_{11}Fe$ and $3.7 \pm 0.3 \times 10^{-11}$ mol cm^{-2} for $SiW_{11}Co$. These values are somewhat lower than 1.0×10^{-10} mol cm^{-2} obtained for $(PMo_{12}/PDDA)_n$ by Wang et al. [50] which they attributed to monolayer coverage, ours corresponding to sub-monolayer coverage. In fact, surface coverage values are highly influenced both by the method and/or polymer used since for the same POMs, depending on these two factors, completely different values were obtained. For example, for $SiW_{11}Co$, they range from sub-monolayer coverage to more than one monolayer [25, 26, 44].

The pH of the electrolyte solution has a clear effect on the voltammetric behaviour. On increasing the pH, from 3.0 to 4.5, the tungsten peak potentials shift to more negative values, giving straight lines with slopes between −63 and −71 mV/pH unit for $SiW_{11}Fe$ ($0.999 \geq r \geq 0.993$) and between −55 and −61 mV/pH unit for $SiW_{11}Co$ ($0.997 \geq r \geq 0.995$). The dependence on pH shows that the reductions involve an equal number of electrons and protons so that the tungsten redox processes in both metal-substituted anions are two-electron/two-proton global processes.

The stability of POM-doped PBCB-modified electrodes was studied by cycling 100 times in pH 4.0 acetate buffer solution between −1.0 and 0.6 V at 50 mV s^{-1}. The peak currents for $SiW_{11}Fe$ decreased by 0.19% after 50 cycles and by 8.4% after 100 cycles. The corresponding values for $SiW_{11}Co$ were 0.14% and 1.4%, respectively. The slight decrease after 50 cycles may be due to the partial depletion of POM in the film on the electrode surface with continuous cycling.

The electrochemical behaviour of polyoxometalates in polymer matrices is, in many cases, similar to that of the same anions in solution [1], as found in this work. Previous reports on $SiW_{11}Fe$ or $PW_{11}Fe$ polymer-doped electrodes are in agreement with this observation. The former has been incorporated into polypyrrole films [51], whereas studies with the latter used polypyrrole, polyaniline, polythiophene and derivatives [52–55]. Cyclic voltammograms show two tungsten and one iron redox peak, which in most cases are surface-confined processes [53, 54], but electrocatalytic properties and stability vary with the system studied.

As mentioned above, the redox activity of the Fe^{III}/Fe^{II} pair could not be studied due to the polymer peaks in the same region of potential. For the cobalt-substituted species, no cobalt reduction/oxidation peaks were expected within the potential range employed, common to what is usually found in aqueous solutions. The reduction of Co^{II} was seen in a previous study with $SiW_{11}Co$ anion incorporated into PEDOT-modified electrodes [44], attributed to the possible interaction between cobalt and the thiophene rings which could stabilise cobalt in a low oxidation state. The different chemical structure of PBCB does not permit this possibility.

Electrochemical impedance spectroscopy of the POM-doped PBCB films

Electrochemical impedance spectroscopy (EIS) was used to examine the interfacial properties of the POM-doped PBCB-modified electrodes. Spectra were recorded at potentials in the range of +0.2 to −0.9 V vs Ag/AgCl in acetate buffer pH 4.0, chosen to encompass the redox reaction of the polymer and polyoxometalate. Figure 3a, b shows complex plane impedance spectra for PBCB/SiW_{11}Fe- and PBCB/SiW_{11}Co-modified electrodes, respectively. For both POMs studied, the behaviour was similar.

The spectra were fitted to two equivalent circuits. For potentials from 0.2 to −0.2 V and at −0.8 V, the spectra are straight lines and the fitting circuit (Fig. 3c) comprises a cell resistance, R_Ω, in series with constant phase element (CPE), modelled as a non-ideal capacitor, given by $\mathrm{CPE} = -1/(Ci\omega)^n$, where C is the capacitance, which describes the charge separation at the double layer interface, ω is the frequency in rad s^{-1} and the n exponent is due to surface heterogeneity. The other circuit is the first one plus an additional resistance, R_{ct}, in parallel with the constant phase element, the charge-transfer resistance at the film/solution interface. These two circuits have been used for PBCB-modified electrodes [42], and the first was also used for POM-doped PEDOT films at −0.3 V [44].

The cell resistance was ~77Ω cm^2 in acetate buffer electrolyte solution for the two POMs studied. Table 2 shows the values of the parameters obtained; in all cases, the error in the fitted values was less than 5%. For both $SiW_{11}Fe$ and $SiW_{11}Co$, the values of capacitance increased from +0.2 to −0.1 V, more so for $SiW_{11}Fe$, then became smaller again until −0.6 V and larger at −0.8 V. The higher values of capacitance correspond to the potentials at which the oxidation/reduction reactions of the polymer and polyoxometalate occur. R_{ct} can be related directly to access to the substrate in the modified electrode and is only manifested in the potential range where there is no redox reaction, with highest values around −0.3 V, indicating that at the potentials where the redox processes of PBCB and POMs take place, charge transfer occurs freely.

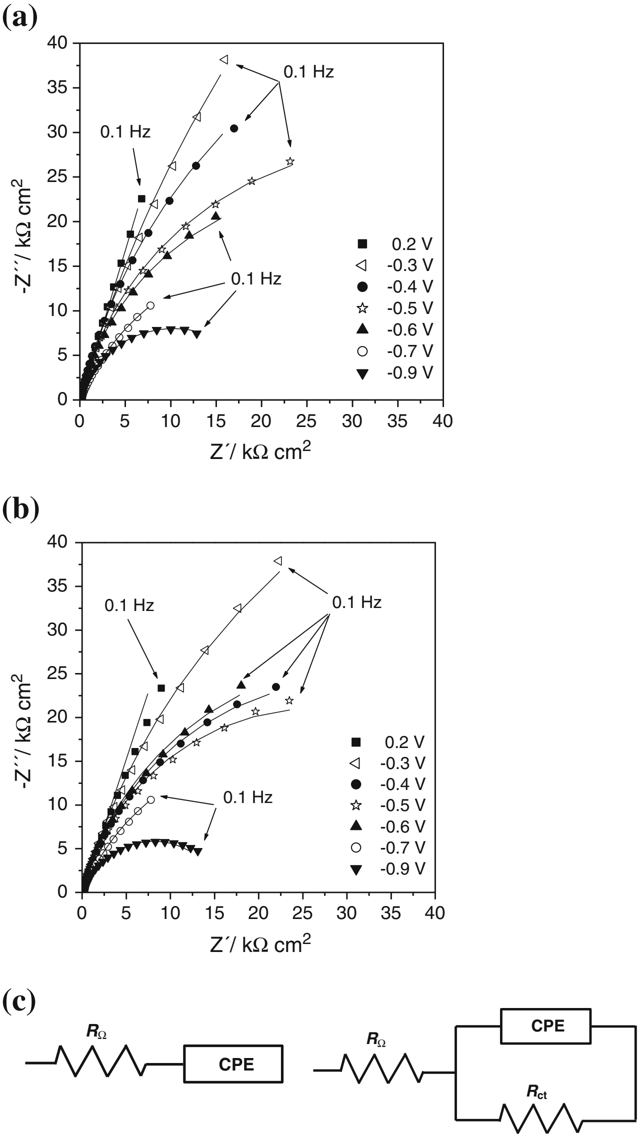

Fig. 3 Complex plane impedance spectra in acetate buffer solution pH 4.0 at different applied potentials of **a** PBCB/SiW_{11}Fe- and **b** PBCB/SiW_{11}Co-modified electrodes; *lines* show equivalent circuit fitting. **c** Equivalent circuits used to fit the spectra

To our knowledge, only one EIS study has been performed using polyoxotungstates incorporated in conducting polymers [44]. The comparison of the impedance spectra of the electrodes described here with those for the same POMs with PEDOT [44] shows that at similar potentials, the spectra for the two types of POM/polymer-modified electrode are different. Those with PEDOT include a linear part at lower frequencies attributed to a diffusion process that is absent in the POM-doped PBCB-modified electrodes since PBCB is a redox polymer where charge has to move between redox centres within the film, whereas PEDOT is a conjugated polymer. However, for POM-doped PEDOT-modified electrodes, charge transfer does not occur freely at

Table 2 Parameters obtained from the impedance spectra of the POM-doped PBCB-modified electrode in pH 4.0 acetate buffer solution by fitting to the equivalent circuit in Fig. 3c

POM	Potential (V vs Ag/AgCl)	C/μF cm^{-2} s^{n-1}	CPE exponent n	R_{ct}/kΩ cm^2
$SiW_{11}Fe$	0.2	63±2	0.82±0.01	–[a]
	0.1	91±1	0.77±0.02	–[a]
	0.0	121±2	0.78±0.01	–[a]
	−0.1	161±3	0.75±0.01	–[a]
	−0.2	44±1	0.82±0.005	–[a]
	−0.3	39±0.5	0.83±0.01	274±2
	−0.4	34±1	0.85±0.01	124±1
	−0.5	32±1	0.84±0.02	69±1
	−0.6	38±0.4	0.85±0.01	59±1
	−0.7	79±1	0.78±0.02	48±1
	−0.8	248±2	0.81±0.01	–[a]
	−0.9	49±1	0.85±0.005	21±0.4
$SiW_{11}Co$	0.2	59±1	0.80±0.005	–[a]
	0.1	79±2	0.75±0.02	–[a]
	0.0	80±1	0.78±0.01	–[a]
	−0.1	81±2	0.76±0.02	–[a]
	−0.2	41±1	0.81±0.005	–[a]
	−0.3	29±0.4	0.83±0.01	149±2
	−0.4	29±1	0.84±0.01	62±1
	−0.5	26±0.4	0.85±0.01	53±0.5
	−0.6	40±1	0.85±0.01	67±1
	−0.7	118±2	0.78±0.02	66±1
	−0.8	252±2	0.80±0.02	–[a]
	−0.9	33±0.5	0.80±0.01	16±0.3

[a] Element not included

the potentials where the POM peaks appear. This can explain the fact that PBCB appears to facilitate charge transfer in relation to PEDOT.

Conclusions

Hybrid films of $[SiW_{11}Fe^{III}(H_2O)O_{39}]^{5-}$ or $[SiW_{11}Co^{II}(H_2O)O_{39}]^{6-}$ with poly(brilliant cresyl blue) have been prepared in aqueous solution by the electropolymerisation of brilliant cresyl blue monomer with the incorporation of the POM anion, on the surface of glassy carbon, with a view to forming a stable matrix for the immobilisation of the POM. This type of polymer has not previously been used for the preparation of POM-modified electrodes. Cyclic voltammograms of the films showed, for both anions, two well-resolved two-electron waves attributable to tungsten redox processes and an additional pair of peaks corresponding to the polymer and that the tungsten reduction processes are surface-confined and proton-dependent. Electrochemical impedance studies showed that PBCB appears to facilitate charge transfer. The modified electrodes are stable, attributed to the electrostatic interaction between the anionic polyoxometalate and the cationic quinone–imine dye brilliant cresyl blue. These results give important information for future studies concerning the possible application of these films in the preparation of electrochemical devices and sensors.

Acknowledgements The authors thank CICECO and the University of Aveiro and CEMUC® of the University of Coimbra (Research Unit 285, FCT), Portugal. Diana Fernandes acknowledges FCT for her PhD grant SFRH/BD/30797/2006.

References

1. Sadakane M, Steckhan ME (1998) Chem Rev 98:219–237
2. Pope MT (1983) Heteropoly and isopoly oxometalates. Springer, Berlin
3. Kurth DG, Volkmer D, Klitzing RV (2003) In: Decher G, Schlenoff JB (eds) Multilayer thin films: sequential assembly of nanocomposite materials. Weinheim, Wiley
4. Pope MT, Müller A (eds) (2001) Polyoxometalate chemistry: from topology via self-assembly to applications. Kluwer, Dordrecht
5. Coronado E, Giménez-Saiz C, Gómez-Garcia CJ (2005) Coord Chem Rev 249:1776–1796
6. Coronado E, Gómez-Garcia CJ (1998) Chem Rev 98:273–296
7. Clemente-Juan JM, Coronado E (1999) Coord Chem Rev 193–195:361–394
8. Gomez-Romero P (2001) Adv Mater 13:163–174
9. Katsoulis DE (1998) Chem Rev 98:359–387
10. Rhule JT, Hill CL, Judd DA (1998) Chem Rev 98:327–357
11. Keita B, Nadjo L (2007) J Mol Catal A Chem 262:190–215
12. Hill CL, Prosser-McCartha CM (1995) Coord Chem Rev 143:407–455
13. Neumann R (2004) In: Bäckvall JE (ed) Modern oxidation methods. Weinheim, Wiley
14. Neumann R (1998) Prog Inorg Chem 47:317–370
15. Briand LE, Baronetti GT, Thomas HJ (2003) Appl Catal 256:37–50
16. Mizuno N, Yamaguchi K, Kamata K (2005) Coord Chem Rev 249:1944–1956
17. Hill CL (2007) J Mol Catal A Chem 262:2–6
18. Flütsch A, Schroeder T, Grütter MG, Patzke GR (2011) Bioorg Med Chem Lett 21:1162–1166
19. Yamase T (2005) J Mater Chem 15:4773–4782
20. Mizuno N, Yamaguchi K, Kamata K (2011) Catal Surv Asia 15:68–79
21. Liu S, Tang Z (2010) Nano Today 5:267–281
22. Adamczyk L, Kulesza PJ, Miecznikowski K, Palys B, Chojak M, Krawczyk D (2005) J Electrochem Soc 152:E98–E103
23. Fernandes DM, Simões SMN, Carapuça HM, Cavaleiro AMV (2008) Electrochim Acta 53:6580–6588
24. Fernandes DM, Simões SMN, Carapuça HM, Brett CMA, Cavaleiro AMV (2010) J Electroanal Chem 639:83–87
25. Fernandes DM, Carapuça HM, Brett CMA, Cavaleiro AMV (2010) Thin Solid Films 518:5881–5888
26. Fernandes DM, Carapuça HM, Brett CMA, Cavaleiro AMV (2011) J Solid State Electrochem 15:811–819

27. Cheng L, Liu J, Dong S (2000) Anal Chim Acta 417:133–142
28. Zhai S, Chen Y, Wang S, Jiang J (2004) Talanta 63:927–931
29. Cheng L, Dong S (2000) J Electroanal Chem 481:168–176
30. Liu J, Cheng L, Dong S (2002) Electroanalysis 14:569–574
31. Skunik M, Baranowska B, Fattakhova D, Miecznikowski K, Chojak M, Kuhn A, Kulesza PJ (2006) J Solid State Electrochem 10:168–175
32. Kulesza PJ, Skunik M, Baranowskaa B, Miecznikowski K, Chojak M, Karnicka K, Frackowiak E, Béguin F, Kuhn A, Delville M, Starobrzynska B, Ernst A (2006) Electrochim Acta 51:2373–2379
33. Dong S, Jin W (1993) J Electroanal Chem 354:87–97
34. Gómez-Romero P, Lira-Cantu M (1997) Adv Mater 9:144–147
35. Gómez-Romero P, Casan-Pastor N, Lira-Cantu M (1997) Solid State Ionics 101:875–880
36. Siné G, Hui CC, Kuhn A, Kulesza PJ, Miecznikowski K, Chojak M, Paderewska A, Lewera A (2003) J Electrochem Soc 150:C351–C355
37. Fabre B, Bidan G, Fichou D (1992) J Chim Phys Phys-Chim Biol 89:1053–1062
38. Lapkowski M, Bidan G, Fournier M (1991) Synth Met 41:407–410
39. Sauvajol JL, Lereporte JP, Chorro C, Poussigue G (1992) J Phys Condens Matter 4:3179–3193
40. Karyakin AA, Karyakina EE, Schmidt H-L (1999) Electroanalysis 11:149–155
41. Pauliukaite R, Ghica ME, Barsan MM, Brett CMA (2010) Anal Lett 43:1588–1608
42. Ghica ME, Brett CMA (2009) J Electroanal Chem 629:35–42
43. Gao S, Cao R, Yang C (2008) J Colloid Interface Sci 324:156–166
44. Fernandes DM, Brett CMA, Cavaleiro AMV (2011) J Electroanal Chem 660:50–56
45. Fernandes DM, Ghica ME, Cavaleiro AMV, Brett CMA (2011) Electrochim Acta 56:7940–7945
46. Tourné CM, Tourné GF, Malik SA, Weakly TJR (1970) J Inorg Nucl Chem 32:3875–3890
47. Zonnevijlle F, Tourné CM, Tourné GF (1982) Inorg Chem 21:2751–2757
48. Barsan MM, Pinto EM, Brett CMA (2011) Phys Chem Chem Phys 13:5462–5471
49. Couto FARS, Cavaleiro AMV, Pedrosa de Jesus JD, Simão JEJ (1998) Inorg Chim Acta 281:225–228
50. Wang B, Vyas RN, Shaik S (2007) Langmuir 23:11120–11126
51. Shiu KK, Anson FC (1991) J Electroanal Chem 309:115–129
52. Fabre B, Bidan G, Lapkowski M (1994) J Chem Soc Chem Commun 1509–1511
53. Fabre B, Bidan G (1997) Electrochim Acta 42:2587–2590
54. Fabre B, Bidan G (1997) J Chem Soc Faraday Trans 93:591–601
55. Gaspar S, Muresan S, Patrut A, Popescu IC (1999) Anal Chim Acta 385:111–117